ISSN 1063-7834, Physics of the Solid State, 2013, Vol. 55, No. 10, pp. 2037–2042. © Pleiades Publishing, Ltd., 2013.
Original Russian Text © T.V. Drokina, G.A. Petrakovskii, M.S. Molokeev, D.A. Velikanov, O.N. Pletnev, O.A. Bayukov, 2013, published in Fizika Tverdogo Tela, 2013, Vol. 55, No. 10, pp. 1922–1927.

MAGNETISM

Specific Features of the Crystal Structure and Magnetic Properties of the $DyFeTi_2O_7$ Compound

T. V. Drokina[a, b, *], G. A. Petrakovskii[a], M. S. Molokeev[a], D. A. Velikanov[a, b], O. N. Pletnev[b], and O. A. Bayukov[a]

[a] *Kirensky Institute of Physics, Siberian Branch of the Russian Academy of Sciences, Akademgorodok 50–38, Krasnoyarsk, 660036 Russia*

* *e-mail: tvd@iph.krasn.ru*

[b] *Siberian Federal University, pr. Svobodnyi 79, Krasnoyarsk, 660041 Russia*

Received February 12, 2013

Abstract—Results of studying the specific features of formation of the crystal structure and distribution of iron cations over the sites in the $DyFeTi_2O_7$ compound have been presented and the comparison with the $GdGaTi_2O_7$ isostructural compound has been performed. The atomic disorder in the distribution of the Fe^{3+} ions over structural sites in the $DyFeTi_2O_7$ compound is confirmed by the Mössbauer spectroscopy and X-ray diffractometry. The results of magnetic measurements in the low-temperature region have revealed an inflection point in the temperature dependence of the magnetic moment and its dependence on the magnetic prehistory of the sample. The obtained experimental data suggest that there is a spin glass state with freezing point $T_f = 6$ K in the $DyFeTi_2O_7$ compound.

DOI: 10.1134/S1063783413100107

1. INTRODUCTION

The $DyFeTi_2O_7$ compound is a representative of the series of compounds with general formula $RMTi_2O_7$ (M = Fe, Ca; R is a rare-earth ion). It is known that the $RFeTi_2O_7$ compounds are isostructural to the $GdGaTi_2O_7$ compound [1]. According to results of X-ray studies, the $GdGaTi_2O_7$ compound crystallizes in the centrosymmetric orthorhombic space group *Pcnb* at room temperature [1]. Eight $GdGaTi_2O_7$ formula units constitute the unit cell. It is constructed by four-vertex, five-vertex, six-vertex, and eight-vertex oxygen polyhedra; the rare-earth cation is located in the eight-vertex polyhedron; three nonequivalent octahedral sites ($M1$, $M2$, and $M3$) are mixed and occupied jointly by Ti and Ga; tetrahedral sties (t) are occupied with Ga, and the Ga cations can come out of tetrahedra and occupy neighboring sites Ga' and Ga" with coordination of five (f).

Magnetic properties of the $RFeTi_2O_7$ compounds (R = Sm, Gd) are investigated in [2, 3], and the formation of spin-glass magnetic states with freezing points $T_f = 7$ and $T_f = 3$ K, respectively, is shown.

In this article, we report a new $DyFeTi_2O_7$ compound with a spin-glass magnetic state. The results of X-ray diffraction, Mössbauer, and magnetic measurements, which were performed with the goal to investigate the magnetic properties and features of the crystal structure, are presented.

2. SYNTHESIS OF THE SAMPLES AND EXPERIMENTAL TECHNIQUE

2.1. Preparation of the Samples

The $DyFeTi_2O_7$ compound was synthesized by the solid-phase reaction from the mixture of Fe_2O_3, Dy_2O_3, and TiO_2 oxides. The pelleted samples 10 mm in diameter and 1.5–2.0 mm thick were subjected to high-temperature treatment at 1250°C and normal pressure. The synthesis was performed in four stages with intermediate wet milling in alcohol and a repeated pressing procedure. The chemical and phase compositions of the samples were monitored by the X-ray structural analysis and nuclear gamma resonance as well as using an optical microscope. The Fe_2TiO_5 impurity is present in synthesized samples in amount of 3.4%.

2.2. X-Ray Structural Investigation

The powder X-ray diffraction pattern of the $DyFeTi_2O_7$ compound was obtained using a D8 ADVANCE (Bruker) diffractometer with the help of a VANTEC linear detector and CuK_α radiation.

The procedure of a variable scanning rate (VCT) and a variable scanning step (VSS) was used. The exposure time increased as angle 2θ increased, which led to considerable improvement of the recorded X-ray diffraction pattern [4–6]. As a rule, five–eight experimental points should fall into the peak full-width at half-maximum (FWHM). However, the peaks considerably broaden as angle 2θ increases.

Table 1. Main crystallographic characteristics of the $DyFeTi_2O_7$ and $GdGaTi_2O_7$ compounds and experimental parameters

Parameter	$DyFeTi_2O_7$	$GdGaTi_2O_7$ according to the data [1]
Space group	*Pcnb*	*Pcnb*
a, Å	9.8470(1)	9.7804(3)
b, Å	13.5751(2)	13.605(1)
c, Å	7.3652(1)	7.4186(2)
V, Å^3	984.54(2)	987.16(1)
Z	8	8
D_x, g/cm^3	5.737	5.848
μ, mm^{-1}	130.319	225.7
Radiation	Cu-K_α	Mo-K_α
2θ-range, deg	5–140	2–70
Number of reflections	942	6267
Number of refined parameters	73	–
R_{wp}, %	1.018	–
$R_{\exp}$, %	0.573	–
R_p, %	0.979	–
$GOF(\chi)$	1.775	–

Note: V is the unit cell volume, Z is the number of formula units in the cell, D_x is the calculated density, μ is the absorption coefficient, R_{wp} is the weight profile discrepancy factor, $R_{\exp}$ is the expected discrepancy factor, R_p is the profile discrepancy factor, and $GOF(\chi)$ is the goodness-of-fit.

Therefore, the step can be increased in high-angle regions of 2θ in order to decrease the time of the experiment [7]. Further, the experimental data were converted into one XYE file commonly accepted in X-ray diffractometry, which contained coordinates $2\theta_i$, intensity I_i, and standard deviation $\sigma(I_i)$ for each experimental point. The Rietveld refinement, which was implemented in the TOPAS 4.2 program [8], takes into account the standard deviation of each point by means of introducing the weight for each point $w_i = 1/\sigma(I_i)^2$ into the least-squares method (LSM). Thus, an increase in the exposure time for the point leads to a decrease in standard deviation $\sigma(I_i)$ and, as a consequence, to its larger weight w_i in the LSM refinement. In the VCT procedure, the weights of weak high-angle and strong low-angle reflections are leveled, while in the usual experiment, the weights are unequal and we loss the information on the structure, which is contained in the high-angle region.

The experimental X-ray diffraction pattern of the sample under study was obtained according to the VCT/VSS procedure and divided into four parts, namely, 5.0°–38.7° (exposure in the point of 3 s, the step of 0.016°), 38.7°–61.6° (exposure in the point of 9 s, the step of 0.024°), 61.6°–97.5° (exposure in the point of 15 s, the step of 0.032°), and 97.5°–140° (exposure in the point of 24 s, the step of 0.040°). The total experiment duration was approximately 16 h. The experiment was divided into the parts in the XRD Wizard program [7]. The location of the peaks was determined in the EVA program (2004) from the DIFFRAC-PLUS software package supplied by Bruker.

2.3. Mössbauer Measurements

The Mössbauer measurements were performed using an MS-1104Em spectrometer at the Kirensky Institute of Physics, Siberian Branch of the Russian Academy of Sciences, at room temperature with the $Co^{57}(Cr)$ source for powders 5–10 μg/cm^2 thick by the natural iron content. The isomer chemical shifts were measured relative to metallic α-Fe.

2.4. Magnetic Measurements

Magnetic measurements were performed using an MPMS-XL magnetometer at the Siberian Federal University in the temperature range of 2–300 K in the magnetic field of 500 Oe.

3. EXPERIMENTAL RESULTS

Structural properties of the sample were investigated by X-ray diffractometry using the $DyFeTi_2O_7$ powder. The difference X-ray diffraction pattern is presented in Fig. 1. The data of the X-ray study indicate that the synthesized $DyFeTi_2O_7$ material has the orthorhombic crystal structure with space group *Pbcn*.

Since the $DyFeTi_2O_7$ compound under study is isomorphic to the $GdGaTi_2O_7$ compound [1], the $GdGaTi_2O_7$ structure was taken as the initial model of the crystal structure. The site occupancies of Ti and Fe atoms were refined under the assumption that the sites are occupied completely while their thermal parameters are fixed. In order to tend the summary cell charge to zero as a result of refinement, we used one soft limitation in a form of the linear equation on the site occupancies of the Ti ions: occ(Ti1) + occ(Ti2)/2 + occ(Ti3) = 2. The results of refinement of occupancies of the $DyFeTi_2O_7$ sample are presented in Table 1. Atomic coordinates, site occupancies p, and thermal parameters B_{iso} of the $DyFeTi_2O_7$ compound are listed in Table 2. The site occupancies p_1 in the $GdGaTi_2O_7$ compound according to data [1] are also presented in Table 2 for comparison.

Refinement of unit cell constants and the analysis of the data showed that parameter a (9.8470) Å in the $DyFeTi_2O_7$ lattice is increased, while parameters b (13.5751) Å and c (7.3652) Å are decreased compared with the $GdGaTi_2O_7$ compound, i.e., a disproportionate variation in parameters of the orthorhombic cell is observed.

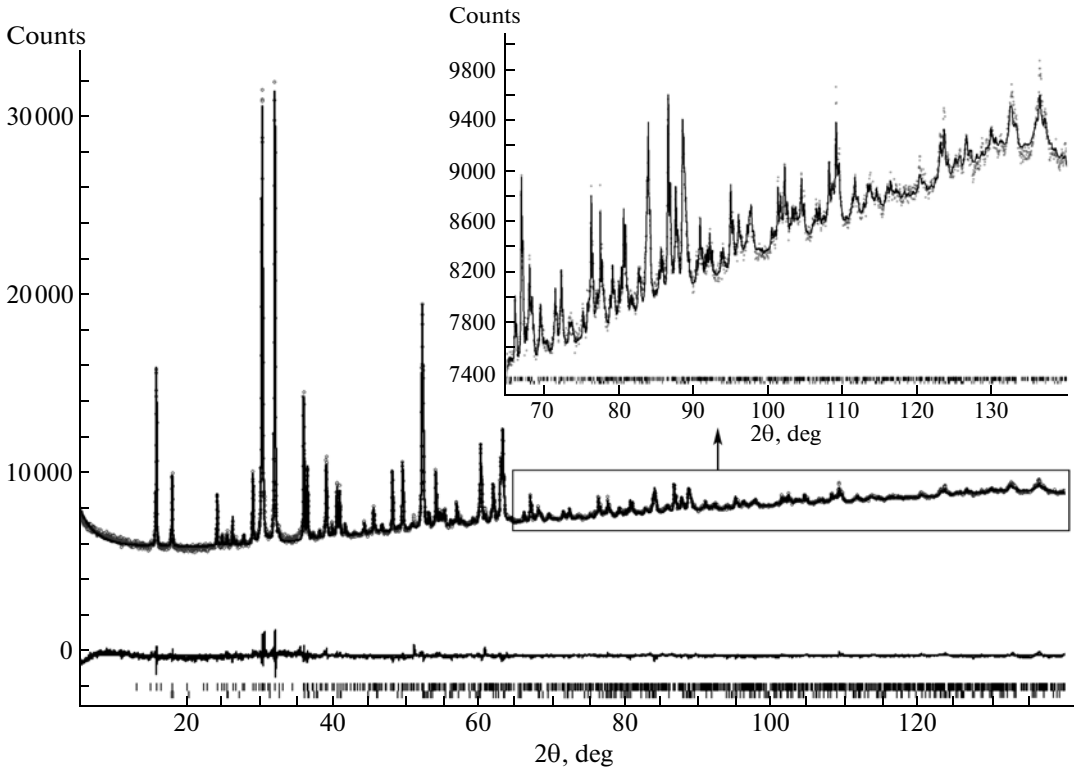

Fig. 1. Room-temperature X-ray diffraction pattern of the $DyFeTi_2O_7$ compound. The difference X-ray diffraction pattern is shown in the lower curve. The substance under study contains 3.4% of the Fe_2TiO_5 impurity.

According to the data of the X-ray investigation, there are five nonequivalent iron (gallium) sites both in the $GdGaTi_2O_7$ lattice and in the $DyFeTi_2O_7$ lattice. However, the experience shows a substantial difference in distribution of titanium; and, correspondingly, of iron; in mixed octahedral sites in isostructural compounds. Populations of titanium in the *M*2 site differ especially strongly: $p_1 = 0.79$ for $GdGaTi_2O_7$ and $p = 0.49$ for $DyFeTi_2O_7$. Thus, in addition to variations in lattice constant, the variation in populations of iron compared with gallium over mixed sites Fe(Ga) and Ti is observed.

Crystal lattice of the $DyFeTi_2O_7$ compound is presented in Fig. 2.

In general, the lattice contains $0.82 \times 8 + 0.49 \times 4 + 0.87 \times 8 = 15.50$ Ti atoms and $0.18 \times 8 + 0.51 \times 4 + 0.13 \times 8 + (0.78 \times 4 + 0.11 \times 8) = 8.52$ Fe atoms. In general, allowing for the standard deviations, the summary formula can be written in the form $DyFe_{1.07(6)}Ti_{1.93(6)}O_7$.

To evaluate the state of iron in $DyFeTi_2O_7$, we performed room-temperature Mössbauer measurements. The Mössbauer spectrum (Fig. 3a) is a sum of overlapping quadrupole doublets. To determine the composition of the model spectrum, we calculated the probability distribution of quadrupole splittings $P(QS)$ in the experimental spectrum, Fig. 3b. In this case, two groups of doublets with various chemical shifts were used as the starting ones. When calculating $P(QS)$, we adjusted amplitudes of doublets and chemical shifts general for each group of doublets.

The maxima and features in distribution $P(QS)$ indicate the possible nonequivalent iron sites in zirconolite $DyFeTi_2O_7$. The information extracted from distribution $P(QS)$ was used to construct the model spectrum, which was then adjusted to the experimental spectrum upon varying the entire set of hyperfine

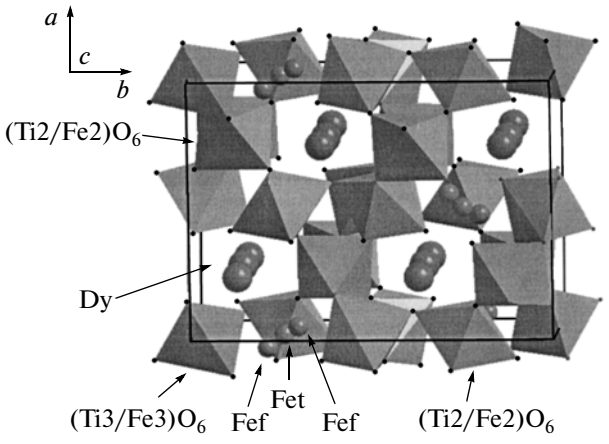

Fig. 2. Crystal structure of the $DyFeTi_2O_7$ compound.

Table 2. Atomic coordinates, site occupancies p, and thermal parameters (isotropic B_{iso} or equivalent B_{eq}) in $DyFeTi_2O_7$ and site occupancies p_1 in the $GdGaTi_2O_7$ lattice

Atom	Site multiplicity	x	y	z	p	B_{iso}/B_{eq}	p_1 [1]
Dy(Gd)	8	0.2465(5)	0.1329(2)	0.0085(5)	1	0.75(4)	1
Ti1	8	0.2492(2)	0.3838(5)	0.487(1)	0.82(2)	1.5	0.88
Fe1(Ga)	8	0.2492(2)	0.3838(5)	0.487(1)	0.18(2)	1.5	0.12
Ti2	4	0.5	0.25	0.255(3)	0.49(6)	1.5	0.79
Fe2(Ga)	4	0.5	0.25	0.255(3)	0.51(6)	1.5	0.21
Ti3	8	0.003(1)	0.4894(7)	0.254(2)	0.87(3)	1.5	0.73
Fe3(Ga)	8	0.003(1)	0.4894(7)	0.254(2)	0.13(3)	1.5	0.27
Fet(Ga)	4	0	0.25	0.331(2)	0.78	1.5(3)	0.78
Fef(Ga)	8	0.037(6)	0.292(4)	0.185(8)	0.11	1.5(3)	0.11
O1	8	0.159(1)	0.391(1)	0.243(5)	1	1	1
O2	8	0.409(2)	0.109(2)	0.249(6)	1	1	1
O3	8	0.103(3)	0.145(1)	0.243(6)	1	1	1
O4	8	0.368(4)	0.286(3)	0.429(5)	1	1	1
O5	8	0.378(4)	0.279(3)	0.051(6)	1	1	1
O6	8	0.373(3)	0.497(2)	0.435(4)	1	1	1
O7	8	0.387(4)	0.475(2)	0.054(5)	1	1	1

parameters of doublets. The result of adjustment is combined in Table 3.

The magnitudes of isomer chemical shifts correspond to cations of trivalent iron Fe^{3+}. Chemical shifts ≥0.3 mm/s are usually observed for Fe^{3+} ions octahedrally coordinated by oxygen, and chemical shifts <0.3 mm/s are characteristic of the tetrahedral coordination.

In order to assign the iron atoms, which were revealed using the Mössbauer procedure, to crystallo-

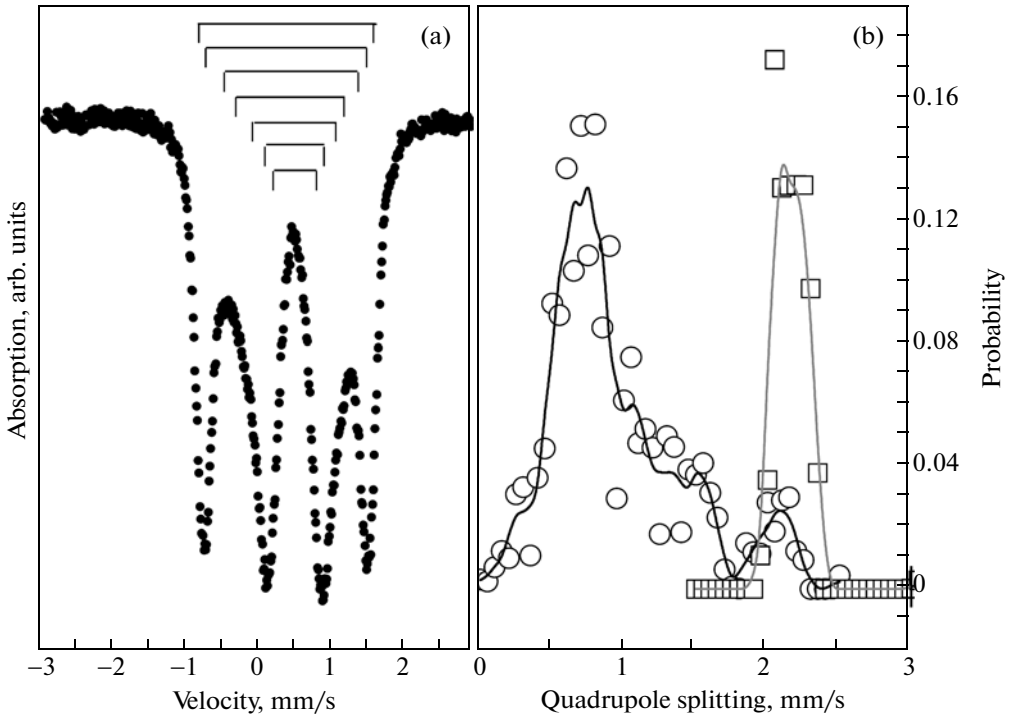

Fig. 3. (a) Mössbauer spectrum of the $DyFeTi_2O_7$ compound at $T = 300$ K and (b) probability distribution of quadrupole splittings in the experimental spectrum.

graphic sites, we used the results of X-ray diffractometry, notably the population of the sites of iron and the degree of distortion of coordination polyhedra. To a first approximation, we can evaluate the distortion of the coordination oxygen polyhedron surrounding the cation under consideration by the magnitude of electric field gradient V_{zz} induced by neighboring oxygen ions. Magnitude V_{zz} should be directly proportional to measured quadrupole splitting QS. We accept that the degree of distortion is $V_{zz} \sim \Sigma(3\cos^2\varphi_i - 1)/r_i^3$, where φ_i is the angle between the main octahedron axis and the direction to the oxygen ion under consideration, and r_i is a distance between the central cation and surrounding oxygen ions.

The gradient calculated based on the X-ray diffractometry data is presented in column V_{zz}^R of Table 3 for all five crystallographic sites of the $DyFeTi_2O_7$ lattice. A quite satisfactory correlation between A and A^R and between QS and V_{zz}^R is seen, based on which, the "Mössbauer" sites of iron are identified in column "Site." Three Fe2 sites; namely, $Fe2_1$, $Fe2_2$, and $Fe2_3$; are revealed in the Mössbauer spectra. This is associated with the chaotic distribution of the Ti cations over the crystal. Three Fe2 sites have various numbers of Ti cations among nearest neighbors. The difference between ion radii of Fe^{3+} (0.67 Å) and Ti^{4+} (0.64 Å) determines the variation in the local distortion at the Fe^{3+} central cation with various numbers of neighboring Ti ions.

Thus, the results of the Mössbauer and X-ray diffractometry studies showed the presence of the atomic disorder in the distribution of the Fe^{3+} ions in zirconolite $DyFeTi_2O_7$.

Figures 4 and 5 show the results of measurement of magnetic properties of the $DyFeTi_2O_7$ compound. Figure 4 shows the temperature dependence of the inverse magnetic susceptibility $\chi^{-1}(T)$ under the condition of cooling the $DyFeTi_2O_7$ sample in field H = 500 Oe. The behavior of curve $\chi^{-1}(T)$ in a higher-temperature region ($T > 50$ K) can be described by the Curie–Weiss law. The Néel asymptotic temperature, which is defined as the intersection point of axis T with asymptote to curve $\chi^{-1}(T)$ in the higher-temperature region, has value $\Theta_N = -19$ K and indicates the preferentially antiferromagnetic exchange interaction in a complex magnetic subsystem of the sample under study. The Curie–Weiss constant $C = 0.036$ K, which corresponds to effective magnetic moment (molar value) $\mu_{eff(exp)} = 11.12\ \mu_B$. The calculated effective magnetic moment of formula unit $Dy^{3+}Fe^{3+}Ti_2O_7$: $\mu_{eff(cal)} = 12.13\ \mu_B$ ($\mu_{eff(cal)}^{Fe^{3+}} = 5.91\ \mu_B$ and $\mu_{eff(cal)}^{Dy^{3+}} = 10.59\ \mu_B$).

The Néel asymptotic temperature Θ_N, the Curie–Weiss constants C in the Curie–Weiss law, as well as the calculated and experimental values of the magnetic moment for the $DyFeTi_2O_7$ compound are presented in Table 4.

Table 3. Mössbauer parameters of the $DyFeTi_2O_7$ compound

IS, mm/s ±0.02	QS, mm/s ±0.02	W, mm/s ±0.03	A, fr. % ±0.03	Site	A^R	V_{zz}^R
0.35	0.59	0.28	0.20	Fe3	0.23	+0.116
0.35	0.81	0.25	0.17	Fe1	0.19	−0.100
0.34	1.14	0.36	0.13	$Fe2_1$		
0.29	1.47	0.49	0.17	$Fe2_2$	0.26	−0.153
0.30	1.83	0.16	0.01	$Fe2_3$		
0.24	2.20	0.25	0.26	Fet	0.25	+0.248
0.23	2.37	0.18	0.06	Fef	0.07	+0.264

Note: IS is the isomer chemical shift relative to α-Fe, QS is the quadruple splitting, W is the line width, A is the fractional site population of iron, A^R is the site population of iron evaluated using the X-ray procedure, and V_{zz}^R is the gradient of the electric field induced by the coordination oxygen polyhedron.

The experimental data also show that the temperature dependence of the magnetic moment of the $DyFeTi_2O_7$ compound under study depends on demagnetization conditions (Fig. 5). As the sample is cooled in the absence of the magnetic field, the temperature dependence of the magnetic moment has the inflection point at $T = 5$ K. The inflection point is not observed upon sample cooling from $T = 300$ K in field H = 500 Oe (upper curve in Fig. 5). Medium curve

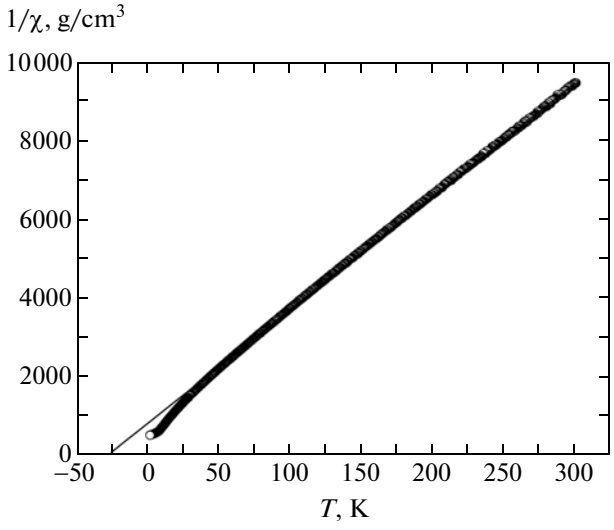

Fig. 4. Temperature dependence of the inverse susceptibility of the $DyFeTi_2O_7$ compound, sample cooling in field $H = 500$ Oe, the Néel asymptotic temperature $\Theta_N = -19$ K.

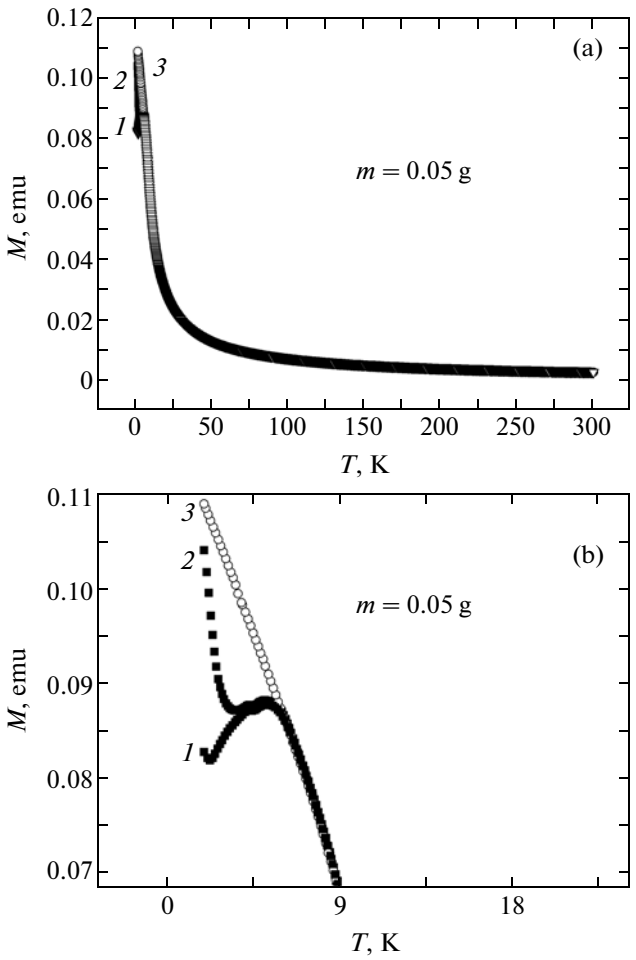

Fig. 5. Temperature dependences of the magnetic moment in the $DyFeTi_2O_7$ compound (a) in the range of 2–300 K and (b) in the lower-temperature region: (*1*) sample cooling in a zero magnetic field (lower curve), (*2*) sample cooling in magnetic field $H = 500$ Oe from temperature $T = 15$ K (medium curve), and (*3*) sample cooling in magnetic field $H = 500$ Oe from temperature $T = 300$ K (upper curve).

corresponds to the case when cooling in field $H = 500$ Oe was performed from $T = 15$ K, which corresponds to the paramagnetic region of the sample under study.

Table 4. Néel asymptotic temperature Θ_N, the Curie–Weiss constants C in the Curie–Weiss law, and the calculated and experimental values of the effective moment for the $DyFeTi_2O_7$ compound

Compound	$DyFeTi_2O_7$
Néel asymptotic temperature Θ_N, K	–19
Curie–Weiss constant C, K	0.036
$\mu_{eff(cal)}$, μ_B	12.13
$\mu_{eff(exp)}$, μ_B	11.12

Thus, there are several values of the magnetic moment depending on cooling conditions of the sample at low temperatures (below freezing temperature $T_f = 6$ K). The results of magnetic measurements are characteristic of the samples with the magnetic state of spin glass. It seems likely that the atomic disorder in the iron distribution in the crystal lattice leads to the formation of spontaneously varying interacting between the atoms below T_f and, possibly, to the presence of competitive magnetic interactions.

4. CONCLUSIONS

The $DyFeTi_2O_7$ compound was synthesized by the method of the solid-phase reaction. The X-ray structural, Mössbauer, and magnetic measurements were performed to determine the magnetic state of zirconolite $DyFeTi_2O_7$ and to refine the structural features.

Allowing for the fractional occupancies of individual sites, the crystal-chemical formula for the compound under study has the form $DyFe_{1.07(6)}Ti_{1.93(6)}O_7$.

Based on the experimental data, which show, on the one hand, the presence of atomic disorder in the distribution of iron ions in the crystal lattice, and on the other hand, the appearance of the magnetic moment at $T > T_f$ and its rise with decreasing temperature down to T_f with the presence of the inflection point near T_f, as well as the dependence of magnetic characteristics on the sample prehistory with the predominantly antiferromagnetic exchange interaction, we can assume that the magnetic state of spin glass is implemented in the $DyFeTi_2O_7$ compound at a temperature below the freezing point $T_f = 6$ K.

REFERENCES

1. E. A. Genkina, V. I. Andrianov, E. L. Belokoneva, B. V. Mill', B. A. Maksimov, and R. A. Tamazyan, Sov. Phys. Crystallogr. **36** (6), 796 (1991).
2. G. A. Petrakovskii, T. V. Drokina, A. L. Shadrina, D. A. Velikanov, O. A. Bayukov, M. S. Molokeev, A. V. Kartashev, and G. N. Stepanov, Phys. Solid State **53** (9), 1855 (2011).
3. G. A. Petrakovskii, T. V. Drokina, D. A. Velikanov, O. A. Bayukov, M. S. Molokeev, A. V. Kartashev, A. L. Shadrina, and A. A. Mitsuk, Phys. Solid State **54** (9), 1813 (2012).
4. I. C. Madsen and R. J. Hill, Adv. X-Ray Anal. **35**, 39 (1992).
5. I. C. Madsen, R. J. Hill, J. Appl. Crystallogr. **27**, 385 (1994).
6. W. I. F. David, NIST Spec. Publ. **846**, 210 (1992).
7. *Diffrac-Plus Basic XRD Wizard* (Bruker, Karlsruhe, Germany, 2002–2007).
8. *General Profile and Structure Analysis Software for Powder Diffraction Data: User's Manual* (Bruker, Karlsruhe, Germany, 2008).

Translated by N. Korovin